Computational Materials Science 152 (2018) 183–191

Contents lists available at ScienceDirect

Computational Materials Science

journal homepage: www.elsevier.com/locate/commatsci

First principles study of phase stability and ferroelectric properties of $Bi_{1-x}RE_xFeO_3$ (RE = Y, La) solid solutions

J. Kaczkowski*

Institute of Molecular Physics, Polish Academy of Sciences, M. Smoluchowskiego 17, 60-179 Poznan, Poland

ARTICLE INFO

Keywords:
Oxide materials
Ferroelectric properties
Multiferroics
Phase transitions
$BiFeO_3$

ABSTRACT

The ferroelectric properties and phase stability of $Bi_{1-x}Y_xFeO_3$ and $Bi_{1-x}La_xFeO_3$ solid solutions have been investigated from x = 0 to 1 using density functional theory. It was found that $BiFeO_3$ undergoes a phase transition from rhombohedral (space group *R*3*c*) to orthorhombic structure at x = 0.15 and 0.32 for Y and La, respectively. Up to x = 0.63 for both systems the polar (space group $Pn2_1a$) and non-polar (space group *Pnma*) orthorhombic phases coexist. For $x > 0.63$ only the non-polar structure is stable. The effect of hydrostatic pressure on the structural and ferroelectric properties of $BiFeO_3$ has been also investigated. The hydrostatic pressure has the same effect on $BiFeO_3$ as Y substitution. The enhancement of the ferroelectric properties of $Bi_{1-x}Y_xFeO_3$ for low x arises from the large off-centering of Y-O atoms, which are caused by the small radius of Y atoms and the mixing of 4d-5p orbitals of Y followed by the hybridization of Y-4d and O-2p orbitals. The calculated ferroelectric polarization for the hypothetical rhombohedral $YFeO_3$ structure is 72 μC/cm^2.

1. Introduction

Bismuth ferrite ($BiFeO_3$ or BFO) has been extensively studied over the past 50 years as the only known room-temperature single-phase multiferroic material (i.e. material with both magnetic and ferroelectric ordering) [1,2,3,4,5]. Magnetic properties of BFO arise from the 3d electrons of the Fe^{3+} ions and ferroelectricity originates from the presence of the stereochemically active $6s^2$ lone pairs on the Bi^{3+} atoms. At ambient conditions BFO crystallizes in a rhombohedral *R*3*c* space group with G-type antiferromagnetic ordering. Despite interesting properties, the commercial applications of $BiFeO_3$ have been hindered due to the high leakage currents and spin-cycloid magnetic ordering. The usual assumption is that the source of the leakage currents in BFO is caused by oxygen vacancies which arise from the variable oxidation state of iron [6–8]. Recent theoretical works based on the density functional theory calculations have shown that the cation-vacancies are dominant defects in BFO under typical processing conditions and could be responsible for the leakage currents and weak ferromagnetism [9–12]. The attempts to overcome these problems and improve the ferroelectric and magnetic properties of BFO can be divided into two categories: (i) optimizing preparation parameters or (ii) ion-doping [1–8,13]. It has been shown that the Bi^{3+} ion substitution by rare earth (RE) elements leads to the reduction of the leakage currents and enhancement of the ferroelectric and magnetic properties [3–6]. Lanthanum is the most widely studied RE dopant in BFO since the early work of Roginskaya et al. [14], and there are numerous experimental results which are often contradictory [15–17] (for review see [4]). For example, in Ref. [15] the remnant polarization of the BFO thin films was increased from 70 μC/cm^2 to 90 μC/cm^2 due to La doping. In addition, the polarization switching and fatigue behavior were also enhanced by the La-doping [15]. On the contrary, in the $Bi_{0.95}La_{0.05}FeO_3$ thin films fabricated by chemical solution deposition technique [16] and sol-gel method [17] the remnant polarization was smaller with respect to the pure BFO films. The remnant polarization decreased from 79 μC/cm^2 to 44 μC/cm^2 in Ref. [16] and from 90 μC/cm^2 to 52 μC/cm^2 [17]. For low La^{3+} doping concentrations (i.e. $x < 0.125$) in $BiFeO_3$ the rhombohedral *R*3*c* structure is preserved [4]. For $x > 0.125$, $Bi_{1-x}La_xFeO_3$ undergo phase transition to orthorhombic structure. Different values of x, up to which the rhombohedral phase is stable are reported, e.g. x = 0.15 [18], x = 0.2 [19–21], x = 0.3 [22–24]. The number of structural phase transitions and the nature of intermediate phases as a function of La doping is still unclear. For example, the phase transition from rhombohedral *R*3*c* phase to orthorhombic $LaFeO_3$-type *Pnma* phase were reported in Refs. [20,23,24]. In contrast, orthorhombic *Imma* symmetry for x = 0.4 with a transition to orthorhombic *Pnma* symmetry for x = 0.5 were reported in Ref. [18]. On the other hand, the phase transitions from rhombohedral *R*3*c* phase to orthorhombic *C*222 phase for x = 0.2 and than to orthorhombic *Pnma* symmetry for x = 0.9 were reported in Ref. [21]. There are also theoretical studies of La-doped $BiFeO_3$ based on the density functional theory

---

* Address: Solid State Division, Institute of Molecular Physics, Polish Academy of Sciences, M. Smoluchowskiego 17, 60-179 Poznan, Poland.
E-mail address: kaczkowski@ifmpan.poznan.pl.

https://doi.org/10.1016/j.commatsci.2018.05.043
Received 2 January 2018; Received in revised form 8 May 2018; Accepted 21 May 2018

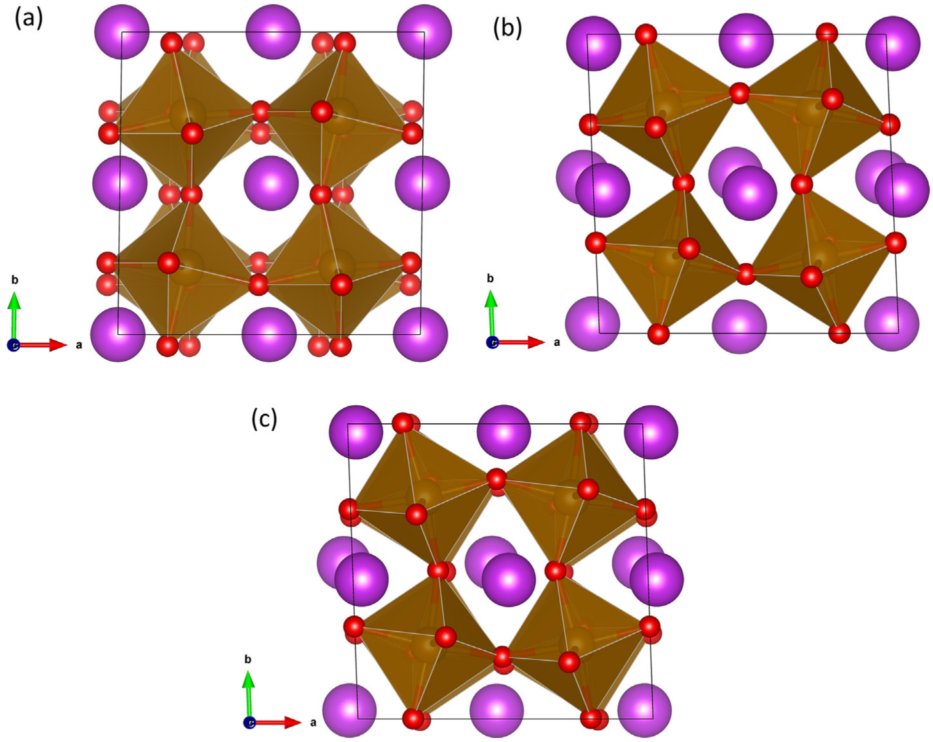

Fig. 1. The three considered 40-atom supercells of $BiFeO_3$: (a) *R*3*c*; (b) *Pnma*; (c) *Pn*2_1*a*.

[25–28]. The solid solution was studied in Refs. [25,26]. The first principle calculations suggest that in the undoped $BiFeO_3$ the total energy differences between the rhombohedral *R*3*c* and two orthorhombic phases i.e. non-polar *Pnma* and polar *Pn*2_1*a* are relatively low [29,30]. The only difference between these orthorhombic phases is the additional ferroelectric distortion in *Pn*2_1*a* phase. In Ref. [25] it was found that at $x = 0.3$, $Bi_{1-x}La_xFeO_3$ transforms from *R*3*c* to orthorhombic structure. In the range of 0.3–0.65, both phases, i.e. ferroelectric *Pn*2_1*a* and paraelectric *Pnma*, are stable. For $x > 0.65$ only the paraelectric phase should be stable. The presence of the intermediate region between pure *R*3*c* phase and pure *Pnma* phase is consistent with many experimental results (neglecting the type of crystal structure) [18,19,21]. In contrast, in Ref. [26] the phase transformation from *R*3*c* to *Pn*2_1*a* phase was obtained at $x = 0.57$. This result does not agree with the fact that $LaFeO_3$ crystallizes in the non-polar *Pnma* structure.

In contrast to lanthanum, yttrium doped $BiFeO_3$ has attracted attention relatively recently. Probably the first experimental work on Y-doped $BiFeO_3$ was that of Mishra et al. [31]. Since their work, numerous other groups have synthesized $Bi_{1-x}Y_xFeO_3$ system using different methods [32–45]. In general, despite different methods of synthesis the improvement of ferroelectric, magnetic, and photocatalytic properties in Y-doped $BiFeO_3$ samples with respect to undoped ones were observed. For concentration of yttrium below 0.1 the enhancement of ferroelectric polarization was observed [37,38,42]. The presence of secondary phases (e.g. $Bi_2Fe_4O_9$) was reduced [32,33,43]. The reduction of leakage currents was reported in Refs. [37,41]. In most cases the phase transition was observed at yttrium concentration of approximately 0.1 [31–34,37,39,44] and the structure was changed from the rhombohedral phase to the orthorhombic one [34,35,37,39,42,44]. The space group of these orthorhombic phases is unclear. In Refs. [35,37] the polar *Pn*2_1*a* space group was observed. On the other hand, the non-polar *Pnma* space group was reported in Refs. [34,39,44]. There are also single reports suggesting phase transition from *R*3*c* to tetragonal structure [31] and from *R*3*c* to *R*-3*m* [38].

From the theoretical side, the solid solution of $Bi_{1-x}Y_xFeO_3$ was not studied so far. The effect of Y substitution on the structural and electronic properties of $BiFeO_3$ were studied using density functional theory calculation by Zhang et al. [27]. In their work, one of the Bi atom in 80-atom supercell was replaced with one Y atom, which correspond to a doping concentration of 6.25% Y. They found that this substitution leads to significant ferroelectric distortion. This effect was attributed to the small ionic size and large electronegativity of Y ion. However, the value of the ferroelectric polarization was not given.

Finally, from the application point of view, the most interesting are materials near the structural phase transition, so-called morphotropic phase boundary. In this region the coexistence of two distinct phases very often lead to the enhancement of electromechanical properties and made possible to control the phase transition through external electric field. In $BiFeO_3$ the morphotropic phase boundary can be induced by strain [46–48] or RE-doping [29,49]. In RE-doped $BiFeO_3$ the structural phase transition can be universally achieved by controlling the average ionic radius of the A-site cation [29]. In La-doped $BiFeO_3$ the formation of straight stripe mixed-phase patterns was observed [50]. The formation of mixed phases at nanoscale level was also observed in strained Y-doped $BiFeO_3$ and, as a result, the high dielectric response was obtained [40].

In this work we investigate the structural, electronic, and ferroelectric properties of $Bi_{1-x}Y_xFeO_3$ and $Bi_{1-x}La_xFeO_3$ systems, with x from 0 to 1 with a step of 0.125, using density functional theory. We also study the undoped $BiFeO_3$ under hydrostatic pressure, and compare the effects of both hydrostatic and chemical pressures on $BiFeO_3$. The main purpose of this study is to investigate $Bi_{1-x}Y_xFeO_3$ compound, which was not previously studied theoretically. The calculations for $Bi_{1-x}La_xFeO_3$ solid solution were performed to clarify the differences between results presented in Ref. [25] and those from Ref. [26]. We would also like to compare the properties of Y- and La-doped $BiFeO_3$ using the same parameters in our density functional calculations and to emphasize the differences between these two compounds.

This work is organized as follows: in the next section the description of the method of calculations is presented, further we present results and discussion, and finally short summation is given.